2009-12-01

Energy Efficiency of Hydrogen Sulfide Decomposition in a Pulsed Corona Discharge Reactor

Morris D. Argyle
mdargyle@byu.edu

Sanil John

Jerry C. Hamann

Suresh S. Muknahallipatna

Stanislaw Legowski

Original Publication Citation

S. John, J.S. Hamann, S. Muknahallipatna, S. Legowski, J.F. Ackerman, M.D. Argyle, "Energy efficiency of hydrogen sulfide decomposition in a pulsed corona discharge reactor." Chemical Engineering Science, 64, 4826-4834, 29. http://www.sciencedirect.com/science/journal/9259/64/23

BYU ScholarsArchive Citation

Energy Efficiency of Hydrogen Sulfide Decomposition in a Pulsed Corona Discharge Reactor

Sanil John,[1] Jerry C. Hamann,[2] Suresh S. Muknahallipatna,[2] Stanislaw Legowski,[2] John F. Ackerman[1], and Morris D. Argyle[1*]
(1) Department of Chemical & Petroleum Engineering, (2) Department of Electrical & Computer Engineering, University of Wyoming, 1000 E. University Avenue, Laramie, WY 82071

Abstract

A novel pulsed corona wire-in-tube reactor with quartz view-ports allowed visual observation of the effect of charge voltage and gas composition on the corona distribution. The H_2S conversion and energy efficiency of H_2S decomposition in this pulsed corona discharge reactor varied at constant power due to the selected values of the electrical parameters of pulse forming capacitance, charge voltage, and pulse frequency. Low pulse forming capacitance, low charge voltage, and high pulse frequency operation produce the highest energy efficiency for H_2S conversion at constant power. H_2S conversion is more efficient in Ar-N_2 gas mixtures than in Ar or N_2. These results can be explained by corona discharge observations, the electron attachment reactions of H_2S at the streamer energies, and a proposed reaction mechanism of H_2S dissociation in the Ar-N_2 gas mixture. The energy consumption per molecule of converted H_2S in an equimolar mixture of Ar and N_2 is the lowest that has been reported for any plasma reactor operated at non-vacuum pressures. The results reveal the potential for energy efficient H_2S decomposition in pulsed corona discharge reactors.

Keywords

Hydrogen sulfide dissociation; Nonthermal plasma; Pulsed corona discharge; Energy efficiency; Hydrogen production

* Corresponding author. E-mail: mdargyle@uwyo.edu, tel: 307-766-2973, fax: 307-766-6777

1. Introduction

The annual demand for hydrogen in the U.S. chemical and refining industries for 2005 was about 8.2 million metric tons (2005), mainly for use as a reactant in the synthesis of ammonia and methanol and in petroleum hydrodesulfurization, hydrocracking, and upgrading processes. Merchant hydrogen production for use in refineries and chemical plants was about 1.4 million metric tons per year (2005). Although the total hydrogen consumption is growing at about 4 percent annually, growth in the merchant hydrogen business is higher, estimated to be about 10 percent, as refineries shift away from captive hydrogen production (2008). With the cost of sweet crude oil increasing, refineries are processing more heavy sour crude, which requires additional hydrogen for sulfur removal. Legislation limiting sulfur content in gasoline and diesel require more hydrotreating process steps in refineries. In addition, as hydrogen is being developed as an energy carrier, the predominant hydrogen production method, steam reforming of natural gas, may be insufficient for future needs. For example, by 2040, the use of hydrogen in fuel cell powered cars and light trucks is anticipated to require annual production of approximately 136 million metric tons of hydrogen (2004).

Hydrogen sulfide (H_2S) is a common contaminant (from ppm concentrations to 90% by volume) in many of the world's natural gas wells. In natural gas processing, it is viewed as a pollutant because it corrodes pipelines and deactivates metal-based catalysts used in steam methane reformation (Huang and T-Raissi, 2008). Traditionally, H_2S is converted via the Claus process to sulfur and water, resulting in a loss of the hydrogen content of the H_2S as low-grade steam. H_2S would be more economically valuable if

both hydrogen and sulfur could be recovered. We estimate the U.S. H_2S production rate from natural gas plants and oil refineries to be on order of 10 million metric tons per year. The theoretical energy required to produce hydrogen from H_2S is only 20.63 kJ/mol H_2 as compared to 63.17 kJ/mol H_2 for steam methane reforming and 285.83 kJ/mol H_2 for water electrolysis, all calculated from standard heats of formation at 298 K (Smith and Van Ness, 1987). Therefore, H_2S represents a significant potential future source of low-cost hydrogen, if efficient processes are developed to extract and recover the H_2.

H_2S decomposition in various types of plasma reactors has been investigated as a method to recover the H_2. Unfortunately, the reported energy consumptions are much higher than the theoretical energy requirement of 0.21 eV per decomposed H_2S molecule (20.63 kJ/mol H_2). All but one of the reported efficiencies exceed the energy requirement of 3.6 eV per H_2 molecule produced required for conventional steam methane reforming, the predominant hydrogen production method, with all separation equipment included (Cox et al., 1998). Dalaine et al., (1998a,b) investigated H_2S conversion in gas systems with concentrations of 0–100 ppm H_2S in air using gliding arc discharges. This type of reactor is rather inefficient, with an energy consumption of 500 eV/H_2S molecule dissociated. A large amount of work on microwave decomposition of H_2S was carried out in the former Soviet Union (Asisov et al., 1985; Bagautdinov et al., 1992, 1993a,b, 1995, 1998). Very low energy consumptions of 0.76 eV/H_2S were reported in both laboratory and pilot units used for the decomposition of pure H_2S or mixtures with CO_2. Encouraged by these reports of high conversions and low energy requirements, a joint project for H_2S conversion using microwave plasmas was undertaken by the Alberta Hydrogen Research Program, Atomic Energy of Canada, and Shell Canada Limited.

Unfortunately, this group reported the energy consumption for H_2S conversion to be about ~4.5 eV/H_2S (Cox et al., 1998) and thus was unable to reproduce the low energy consumption reported by the Russian researchers. All microwave plasma experiments for H_2S conversion in the Canadian studies were performed at pressures below 1 atmosphere, which requires additional energy consumption for compression and vacuum costs. Traus and Suhr (1992) and Traus et al. (1993) investigated conversion of H_2S at 10–100 mol% concentrations in Ar, N_2, and H_2 in a silent discharge reactor and in a rotating glow discharge reactor. They found that the energy consumption for H_2S conversion in a rotating glow discharge reactor (~27 eV/H_2S) is less than that in a silent discharge reactor (~81 eV/H_2S). In addition, Abolentsev et al. (1995) and Ma et al. (2001) investigated decomposition of low (ppm) concentrations of H_2S in different balance gases, including air, N_2, H_2, He, and CH_4, using a silent discharge reactor. H_2S conversion in pulsed corona discharge reactors was also studied by several investigators (Averin et al., 1996; Helfritch, 1993; Ruan et al., 1999; Wiseman and Douglas, 1972). These investigations were conducted at low H_2S concentrations (<2 mol %) with high (>100 eV/H_2S) energy consumption, which are not practical conditions for commercial application.

We previously reported the lowest energy consumption of 17.4 eV/H_2S molecule for moderately high concentrations of H_2S, 16% H_2S in Ar, (Zhao et al., 2007) at non-vacuum pressures (134 kPa). Also, at higher H_2S concentrations (>16 mol %), H_2S decomposition in Ar produced higher conversions and reaction rates, as compared to those in He, N_2, and H_2. Therefore, Ar was selected as the balance gas for most of the future experiments. Although Ar can be separated from H_2S and H_2 at the reactor outlet

and recycled to the process, it is relatively expensive compared to N_2. Therefore, Ar diluted with N_2 was also used as a balance gas with improved performance.

The electrical parameters of charge voltage (V_c), pulse frequency (f), and pulse forming capacitance (C_p) have been reported to impact the conversion of various reactants in plasma reactors. For methane conversion, the moles of methane converted per unit of energy supplied decreased with increasing charge voltage and increased with increasing pulse-frequency (Ma et al., 2001), while methane conversion and energy efficiency were higher at a pulse forming capacitance of 1280 pF as compared to 1920 pF at different power inputs (Zhao et al., 2006b). H_2S conversion increased with increasing charge voltage for ppm concentrations of H_2S in an ozonizer (Haas and Khalafalla, 1973). NO conversion at ppm concentrations (Mok, 2000) increased with increasing pulse frequency and capacitance. In all these studies, the total power supplied to the reactor changed as each of these parameters changed because power input is defined as $P = ½C_pV_c^2f$, where C_p is the pulse forming capacitance, V_c is the charge voltage, and f is the pulse frequency. This study reports the effect of these parameters at constant power to isolate the effects on H_2S conversion as these parameters were varied at constant power input.

2. Experimental

The experimental system, shown in Figure 1, consists of a stainless steel reactor, a flow control and distribution system, and an electrical system. The reactor is a vertical wire-in-tube design, with gas flow from top to bottom. The anode is a 0.001 m diameter stainless steel wire passing axially through the center of the cathode tube. The cathode is

a stainless steel tube, 0.024 m in diameter and 0.889 m long, with 7 quartz view-ports and 7 ports for sampling and temperature measurement placed equidistantly along its length. The 0.01 m diameter quartz view-ports permitted visual inspection of the corona discharge. At the same operating conditions, similar H_2S conversions were obtained in geometrically similar cathode tubes, with and without ports, indicating negligible effect of the cathode viewports on the corona discharge. The stems of the bimetallic thermometers were immersed about 0.025 m into tees to be flush with the cathode tube inner wall. The thermometers proved to be unresponsive and displayed near ambient temperatures even when the tube was warm to touch.

Gas mixtures entered the reactor at ambient temperature (~300 K) and a controlled flow rate (1.18×10^{-4} $SCMs^{-1}$). The pressure in the reactor was maintained at 134 kPa by a back pressure regulator. The H_2S in Ar gas mixture was prepared by mixing ultra high purity (UHP) H_2S (Airgas) with UHP Ar (US Welding). The desired entrance mole fraction of H_2S was set with two well-calibrated mass flow controllers (Brooks Mf50x & Mf51x). The reactant and product gases were analyzed with a mass spectrometer (Stanford Research Systems QMS 100 Series Gas Analyzer). To perform quantitative measurements, an internal standard method (Watson, 1997) was used to calibrate the ion signal response at an *m/z* ratio of 34 with the H_2S mole fraction, in which Ar was used as an internal standard. For experiments involving mixtures of nitrogen, UHP N_2 was introduced to the H_2S-Ar mixture by a calibrated rotameter. The mixture compositions used for the H_2S decomposition experiments involving nitrogen are shown in Table 1. The mass spectrometer was calibrated for H_2S concentrations ranging from 4% to 10% in 23% N_2 (balance Ar), 46% N_2 (balance Ar), and 69% N_2 (balance Ar). For

the gas mixture 5 in Table 1, N_2 was used as an internal standard to calibrate the mass spectrometer.

The structure of sulfur deposits in the reactor was analyzed by an X-ray diffractometer (SCINTAG XDS2000 producing Cu K_α X-rays and equipped with a theta-theta goniometer and a solid state X-ray detector).

The reactor electrical circuit diagram is shown in Figure 2. The electrical system produces a positive DC pulsed corona discharge and is capable of delivering charge voltages from 6.9 kV to 30 kV and pulse frequencies from 0 to 1000 Hz. It consists of a high voltage DC power supply, a capacitive energy storage medium, and a hydrogen thyratron connected to the reactor. A 40 kV oil-cooled, high voltage supply charges the capacitor bank, which could be increased in four increments of 720 pF (using TDK FHV-10AN capacitors). The hydrogen thyratron (L-3 Electron Devices Type L-4945) is an electrical switch that uses hydrogen gas as the switching medium. The switching action is achieved by a shift from the insulating properties of neutral gas to the conducting properties of ionized gas. The thyratron is designed to withstand a high voltage in the 'off' state, to trigger at a precisely defined time, to pass high peak current pulses in the 'on' state, and to recover rapidly to the 'off' state to allow high repetition rate operation (2002). When the thyratron triggers, the stored energy in the capacitor bank is discharged in a few nanoseconds to the anode, which creates the plasma in the gas flowing through the reactor tube. The formation of corona discharge can be detected by a discharge waveform recorder (Tektronix TDS 220). The energy released by the capacitors per pulse was calculated as $\frac{1}{2}C_pV_c^2$, where C_p is the pulse forming capacitance in pF, and V_c is the constant charge voltage before discharge in volts. The power consumed, W ($J \cdot s^{-1}$),

was calculated as the product of the input energy per pulse ($½fC_pV_c^2$,) and the pulse frequency (f) in Hz. Tables 2 and 3 show the electrical parameters for the constant power (100 W) experiments and the experiments involving nitrogen, respectively.

The charging capacitors, limiting resistor, hydrogen thyratron switch, and electrical connections to the reactor were all enclosed in Teflon. The Teflon insulation ensures very low stray capacitance in the range of 0.1 to 0.5 pF because of its high dielectric strength. The electrical lines connecting the capacitors, thyratron, and reactor are solid steel rods enclosed in Teflon, again ensuring very low stray capacitance and low inductance.

3. Results and Discussion

3.1. Visual observations of the corona reactor

The corona discharge was visible around the wire through the viewports, as shown in Figure 3. Visual observation confirmed that intensity of the discharge was not uniform along the length of the tube. The corona was not observed in all viewports simultaneously during the discharge duration. The location of the brightest and constant discharge depends on the type of gas, concentration of individual gases in the case of mixtures, and charge voltage. In pure Ar, the brightest and constant discharge occurred in the upper region (0.3-0.6 m from the top of the reactor), while in pure N_2, the discharge occurred in the lower region (0.3-0.6 m from the bottom of the reactor). These observations were interpreted with respect to the molecular structure of these gases, as Ar is monatomic while N_2 is diatomic. As the gases travel through the cathode tube from top to bottom, they interact with the electrons energized by the pulsed electric field

between the wire and the tube. In a monatomic gas, like Ar, electrons predominantly experience elastic collisions with Ar atoms without energy loss, if the electron energy is less than the energy (11.6 eV) (Fridman and Kennedy, 2004d) of the lowest electronically excited state of Ar, $Ar(^3P_2)$. The electrons that experience these elastic collisions are further accelerated and hence gain more energy in the electric field. When electron energy exceeds the excitation energy (11.6 eV) required to excite ground state argon to $Ar(^3P_2)$, the electrons may experience inelastic collisions and lose kinetic energy. In contrast, when energetic electrons collide with diatomic molecules, like N_2, the electrons may lose energy through many other processes unavailable to monatomic species, such as dissociation (10 eV) (Ma et al., 2001), electronic excitation of lower energy transitions (~6.1-12 eV) (Zhao et al., 2004), rotation (~10^{-4}-10^{-5} eV) (Fridman and Kennedy, 2004c), and vibration (1.7-3.5 eV) (Fridman and Kennedy, 2004c), depending on the electron energy. This implies that electron energy cannot be accumulated in diatomic balance gases to the same levels as in monatomic gases. Therefore, diatomic gases, such as N_2, have to travel further through the applied electric field within the tube before a corona discharge can occur. Hence, the brightest discharge in N_2 takes place lower in the reactor than in Ar. This explanation also describes the observed downward shift of the brightest discharge in Ar on dilution with a polyatomic gas like H_2S.

In an earlier study of positive streamers in ozone for a wire-plate pulsed corona discharge system (Winands et al., 2006), the thickness, intensity, and velocity of primary streamers increased as the applied voltage increased. The number of streamers leaving the anode also increased, but the number reaching the cathode was independent of voltage. In the same study, pulse frequencies up to 400 Hz had no effect on the diameter,

intensity, and number of streamers. This implies an increase in primary streamer volume with voltage which could potentially increase conversion. Although we did not measure the thickness, intensity, and velocity of streamers, we observed that the number of viewports where corona could be seen decreased with an increase in the charge voltage. As charge voltage is increased from 11 kV to 21 kV, the discharge moved from the lower portion of the reactor to the upper portion. This increase in voltage causes an increase in the electric field around the wire, which imparts more energy to the electrons, causing the corona discharge to occur earlier as the gas flows from top to bottom. At lower voltages (11 kV, 13 kV & 15 kV), the corona discharge was observed through 2, 3, or even 4 view ports in the middle and lower regions of the reactor, while the remaining view ports were dark. At higher voltages (17 kV, 19 kV & 21 kV), the corona was seen only in the upper region through 1 or 2 view ports. This indicates that the plasma volume in the reactor increases with decreasing voltage and increasing frequency. Thus, the reactor volume is used more efficiently in this condition as indicated by an increase in conversion, discussed below.

3.2. H_2S conversion in Ar increases with decreasing charge voltage and increasing pulse frequency at constant pulse forming capacitance and power

Figures 4(a) and 4(b) show the effect of increasing charge voltage on H_2S conversion for four different values of capacitance. Figure 4(a) contains data for 8 mol% H_2S in Ar, while Figure 4(b) contains data for 12 mol% H_2S in Ar. For any particular value of capacitance, the H_2S conversion decreased with increasing charge voltage, which corresponds to decreasing pulse frequency at a constant power input of 100 W. High pulse frequency and low charge voltage conditions were the best for H_2S

conversion for all values of pulse forming capacitances. The highest conversions obtained were 27.7% for the 8% H_2S-92% Ar and 24.9% for the 12% H_2S-92% Ar mixtures. The proposed explanation for this behavior is based on the energy of electrons in the streamers.

In pulsed corona discharges in air and flue gas, a difference in the streamer characteristics with increasing charge voltage has been reported (Yan et al., 1998). Streamers are thin ionized luminous channels formed between the electrodes. They are of two types: primary and secondary. For our case with a positive pulsed corona discharge, the streamers propagate from the wire (anode) to the tube (cathode) within tens of nanoseconds. The primary streamers carry high energy electrons (~10 eV), while secondary streamers carry low energy electrons (~1-3 eV) (Winands et al., 2006). Secondary streamers develop when the primary streamers approach the cathode (Yan et al., 1998). With increasing charge voltage, the average streamer propagation velocity increases, resulting in a decrease in the duration of primary streamer propagation (Yan et al., 1998). This increase in streamer velocity due to increasing voltage is supported by the decrease in duration of the primary streamer discharge observed in the discharge voltage waveform during methane conversion in a pulsed corona discharge reactor (Yao et al., 2001). As the primary streamers die out faster with increasing voltages, the secondary streamers start developing at higher voltages. Thus, at higher charge voltages, both primary and secondary streamers are formed, while at lower charge voltages, only primary streamers are formed. This behavior has been reported in both wire-plate and wire-cylinder reactors, irrespective of power system specifications (Yan et al., 1998). Therefore, the low charge voltage condition produces more electrons with an average

energy of 10 eV, which is closer to the excitation energy (11.6 eV) for the lowest electronically excited state of Ar (Ar($^3P_2$)) and higher than the electron energy range (8-9 eV) in which the maxima in the absolute total electron-scattering cross section for H_2S occurs ($\sigma_{max} = 40 \times 10^{-20}$ m^2) (Szmytkowski et al., 2003). These electron energies are more than sufficient for dissociation of H_2S into HS and H because the H-SH bond strength at 298 K is 3.96 eV (Lide, 2003). Excitation of Ar and direct dissociation of H_2S by electron impact have been proposed as the two initiating mechanisms responsible for H_2S decomposition in Ar (Zhao et al., 2007).

The rates of dissociative electron attachment reactions of H_2S are higher with electrons in the secondary streamer than with electrons in the primary streamer. The dissociative electron attachment reactions of H_2S with the low energy (~1-3 eV) electrons of the secondary streamers and the high energy electrons (~10 eV) of the primary streamers are shown in Table 4 (Rao and Srivastava, 1993). These processes are likely in our reactor because the appearance potentials of the ions (defined as the minimum energy of the electrons in the ionizing beam necessary to produce a given fragment ion) are lower than or approximately equal to the energy of the electrons in the streamer. The approximate cross sections shown in Table 4 correspond to the energies of electrons in the primary and secondary streamers. HS^- formation due to dissociative electron attachment processes occurs at a faster rate (2 orders greater, based on the data in Table 4) within secondary streamers due to its greater cross section, while S^- formation will occur at similar rates compared to the reactions in the primary streamers. Such electron attachment processes are considered essential in weakly ionized plasmas, like corona discharges, with low electron concentrations and low degrees of ionization and are first

order with respect to electron concentration (Fridman and Kennedy, 2004b). As these processes capture electrons and decrease their concentration, the rates of electron collision reactions decrease, as observed previously (Zhao et al., 2005b,c) and may reduce H_2S decomposition rate, as suggested previously (Zhao et al., 2007). In the primary streamers, the decrease in electron concentration by dissociative electron attachment is more than compensated by the direct electron collision ionization of H_2S leading to H_2S^+ production. The cross section of this ionization process is at least two orders of magnitude higher than that of the electron attachment processes in primary streamers (see Table 4). Other positive ion formation by electron-impact dissociative ionization is unlikely in our reactor because the appearance potentials for HS^+, S^+, H^+, H_2^+, H_2S^{++}, and S^{++} ions are 14.35 eV, 13.45 eV, 15.50 eV, 16.50 eV, 32.00 eV, and 40.50 eV, respectively (Rao and Srivastava, 1993), which are all significantly greater than the average energy (10 eV) of electrons in the primary streamer.

Energy efficiency has previously been suggested to decrease with secondary streamer formation. For example, for ppm-concentration SO_2 removal in pulsed corona discharges, the energy utilization efficiency decreased with increasing charge voltage (Bingyan et al., 2005). Energy utilization efficiency is defined as the ratio of the primary streamer energy to the total pulse discharge energy. Two peaks have been reported in the discharge voltage, discharge current, and power waveforms from an oscilloscope over the pulse duration. The first and the second peaks represent the primary streamers and the secondary streamers, respectively (Bingyan et al., 2005; Yao et al., 2001). The primary streamer energy is calculated by integrating the first power peak, while the total pulse discharge energy is calculated by integrating the discharge power waveform. Analogous

to SO_2 removal, the observed decrease in conversion (Figure 4) at higher voltages is likely due to additional energy being used in secondary streamer formation, thereby reducing the energy utilization efficiency.

In these experiments, any increase in charge voltage is accompanied by a decrease in pulse forming frequency to keep the input power constant. Consistent with the data shown in Figure 4, the decrease in conversion at higher charge voltages is likely caused by formation of energy-inefficient secondary streamers. Thus, although the power supplied to the pulsed corona reactor is the same, low voltage and high frequency operating conditions are desirable for H_2S decomposition to maximize energy efficiency by minimizing secondary streamer formation.

3.3. Energy consumption for H_2S conversion in Ar decreases with decreasing pulse forming capacitance at constant power.

Figure 5 shows the energy consumption per H_2S molecule converted as a function of charge voltage for four values of pulse forming capacitance, again at constant power input of 100 W, for 8 mol% H_2S in Ar (Figure 5(a)) and for 12 mol% H_2S in Ar (Figure 5(b)). The energy consumption decreases with decreasing pulse forming capacitance values at constant power. For example, for the 12% H_2S-88% Ar mixture, at a constant charge voltage of 17 kV, the energy consumption at 720 pF is only 8.2 eV/H_2S molecule compared to 15 eV/H_2S molecule at 2880 pF. The lowest pulse forming capacitance (720 pF) tested provides the least energy consumption per H_2S molecule converted (9.8 eV/H_2S for the 8% H_2S-92% Ar mixture and 7.3 eV/H_2S for the 12% H_2S-88% Ar mixture), which corresponds to the highest energy efficiency. This phenomenon can be

explained by the optimum energy transfer condition proposed by Uhm and Lee (1997) and by Mok (2000).

In their analytical investigation of corona discharge systems, (Uhm and Lee, 1997) reported the optimum energy transfer condition as

$$2\frac{C_e}{C_{R0}} = 1 + 2\frac{\ln(R_0/R_c)}{\ln(1.11\zeta)} \tag{1}$$

where, C_e is the capacitance of the external circuit (pulse-forming capacitance), C_{R0} is the initial capacitance of the reactor chamber, R_0 is the radius of the wire, R_c is the radius of the tube, and ζ is the normalized plasma mobility, which is related to the ionization front velocity. The normalized plasma mobility is proportional to the pulse-forming capacitance and is inversely proportional to the reactor volume.

In Mok's experimental study of ppm-concentration NO decomposition in a wire-plate reactor (Mok, 2000), he calculated the initial capacitance of the reactor (C_{R0}) by measuring the discharge voltage and current, when the charge voltage is lower than the corona onset value, as follows:

$$I_{cap} = C_{RO}\frac{dV}{dt} \tag{2}$$

where, I_{cap} is the measured capacitive current and dV/dt is the rate of change in the discharge voltage. As the charge voltage applied was less than the corona onset value, the measured current was purely capacitive and did not include corona current. Mok found that the reactor capacitance increased and reached a value three times the initial reactor capacitance during the corona discharge. Further, he found that the energy transferred from the pulse-forming capacitance to the reactor reached a maximum when the pulse-forming capacitance was three times the initial capacitance of the reactor. He

verified this by electrical measurements and by the NO decomposition experiment by increasing pulse-forming capacitance. As a result, he proposed the optimum energy transfer condition as,

$$\frac{\text{Pulse - forming capacitance } (C_P)}{\text{Initial capacitance of reactor } (C_{R0})} \approx 3 \tag{3}$$

The initial capacitance of the reactor (C_{R0}) can be calculated using a capacitance formula for the wire-in-tube geometry (Shin et al., 2000):

$$C_{R0} = \frac{2\pi k \varepsilon_0 L}{\ln(R/r)} \approx 16.7\ pF \tag{4}$$

Here, R is the cathode tube radius (0.012 m), r is the anode wire radius (0.00057 m), L is the reactor length (0.914 m), ε_0 is the permittivity of free space (8.854 x 10^{-12} F/m), and k is the dielectric constant of the mixture of H_2S and Ar (~1). For our case of high concentration H_2S decomposition in Ar at constant power, results similar to the ppm-concentration NO decomposition were obtained. However, in the present study, the capacitance was increased to maintain constant power input by decreasing charge voltage and frequency, unlike in Mok's work. Thus, at 720 pF capacitance, a higher fraction of the 100 W of supplied energy is transferred into the reactor, resulting in higher H_2S conversion and lower energy consumption. Table 5 shows representative data of energy consumption as a function of the pulse forming capacitance and the capacitance ratio (pulse forming capacitance/reactor capacitance) for the four values of pulse forming capacitance used in this study. Figure 6 shows the representative data graphically. Although the capacitance ratio for the reactor used in this study is far from the optimum proposed by Mok, the trend of decreasing energy consumption (corresponding to

increasing energy efficiency) as the capacitance ratio approaches the optimum energy transfer ratio is clear.

3.4. H_2S conversion in N_2-Ar mixtures

H_2S conversion is higher in monatomic gases (Ar and He) than in diatomic gases (N_2 and H_2) (Zhao et al., 2007). At high H_2S concentrations (>16%), H_2S conversion in Ar was the highest. However, as Ar is more expensive than N_2, the process could be more economical if Ar were diluted with N_2 and comparable H_2S conversions to that in pure Ar could be obtained. Further, energy efficiency might be further improved by establishing a corona in more of the reactor volume. As noted earlier, the corona was observed only in the upper region of the reactor in a pure monatomic gas (Ar) and only in the lower region in a pure molecular gas (N_2). If it were possible to produce a corona along the entire length of the reactor, the plasma volume would increase which should increase H_2S conversion at a given input power. This hypothesis was explored by mixing a molecular gas (N_2) with a monatomic gas (Ar). H_2S is not a suitable candidate as a molecular gas because of its high dielectric strength (~2.9) (Christophorou et al., 1987) and is already present as the reactant. Therefore, N_2 was mixed with Ar and H_2S to increase plasma volume and H_2S conversion.

H_2S decomposition was performed in various concentrations of Ar and N_2 at three different input power values (60 W, 80 W, and 100 W) to verify repeatability of the results. The H_2S conversion and energy consumption at the three input powers as a function of composition for the four mixtures are shown in Figures 7 and 8, respectively. The H_2S conversion initially increases with increasing addition of N_2, reaches a maximum for the 46% N_2-46% Ar mixture, and then decreases (Figure 7). As the energy

consumption is inversely proportional to the H_2S conversion, energy consumption initially decreases with increasing addition of N_2, reaches a minimum for the 46% N_2-46% Ar mixture, and then increases. Consistent with our earlier experiments (Zhao et al., 2007), the H_2S conversion in N_2 is lower than in Ar. The deviation of conversion for 60 W input power, which for 92% N_2 is slightly higher than that at 80 W input power, is not significant because these data points fall within the experimental uncertainty of +/-10% at a 95% confidence interval.

The location of the brightest and constant discharge and the number of viewports through which corona was observed, changed with the feed gas composition. As the N_2 concentration was increased from zero, the brightest and constant discharge descended. For example, at 100 W, the top two viewports for the 8% H_2S-92% Ar and the 8% H_2S-23% N_2-69% Ar mixtures were lit, while the 5th and 6th viewports were lit for the 8% H_2S-69% N_2-23% Ar and the 8% H_2S-92% N_2 mixtures. More importantly, the number of viewports through which corona was observed, increased from two for the 8% H_2S-92% Ar mixture to five for 8% H_2S-46% N_2-46% Ar mixture, and then decreased to three for 8% H_2S-92% N_2 mixture at 100 W. Therefore, the plasma volume is greatest for the 46% N_2-46% Ar-8% H_2S mixture, filling approximately 70% of the reactor, compared to 40% for the 8% H_2S-92% N_2 mixture and 30% for the 8% H_2S-92% N_2 mixture at 100 W. For the 8% H_2S-46% Ar-46% N_2 feed mixture, the energy consumption was the lowest, at 6.0 eV/H_2S for 100 W, 5.3 eV/H_2S for 80 W, and 4.9 eV/H_2S for 60 W. This value of 4.9 eV/H_2S is the lowest reported value for H_2S decomposition at non-vacuum pressures for any H_2S concentration.

For H_2S-Ar mixtures, our previous investigation (Zhao et al., 2006a) concluded that the major product for direct electron collision with Ar is the lowest excited state of Ar, $Ar(^3P_2)$, which has an excitation energy of 11.55 eV.

$$e + Ar \rightarrow Ar(^3P_2) + e \qquad (R1)$$

The $Ar(^3P_2)$ contributes to H_2S dissociation and H_2 dissociation through Reactions R2 and R3 (Gundel et al., 1976; Velazco et al., 1978).

$$Ar(^3P_2) + H_2S \rightarrow Ar + H + HS \qquad k = 5.18 \times 10^{14}\ cm^3 \cdot mol^{-1} \cdot s^{-1} \qquad (R2)$$

$$Ar(^3P_2) + H_2 \rightarrow Ar + H + H \qquad k = 3.97 \times 10^{13}\ cm^3 \cdot mol^{-1} \cdot s^{-1} \qquad (R3)$$

For H_2S-N_2 mixtures, the major products from electron collision reaction with N_2 are N radicals and the first electronic excited state of N_2, $N_2(A)$, which requires an excitation energy of 6.1 eV (Zhao et al., 2004).

$$e + N_2 \rightarrow N + N + e \qquad (R4)$$

$$e + N_2 \rightarrow N_2(A) + e \qquad (R5)$$

The previous investigation (Zhao et al., 2005a) reported that the rate of electron collision reaction R5 is about 7 times higher than that of R4. These active species react with N_2, H_2S, and H_2 (Aleksandrov et al., 1994; Herron, 1999; Kossyi et al., 1992), according to the following reactions:

$$N + H_2 \rightarrow NH_2 \qquad k = 1.14 \times 10^4\ cm^3 \cdot mol^{-1} \cdot s^{-1} \qquad (R6)$$

$$N + N \rightarrow N_2 \qquad k = 8.54 \times 10^{10}\ cm^3 \cdot mol^{-1} \cdot s^{-1} \qquad (R7)$$

$$N_2(A) + H_2 \rightarrow N_2 + 2H \qquad k = 2.11 \times 10^9\ cm^3 \cdot mol^{-1} \cdot s^{-1} \qquad (R8)$$

$$N_2(A) + H_2S \rightarrow N_2 + H + HS \qquad k = 1.81 \times 10^{14}\ cm^3 \cdot mol^{-1} \cdot s^{-1} \qquad (R9)$$

There are no reports of rate constants for reactions between H_2S and N. However, by analogy to the extremely low rate constant of the reaction between N and H_2O (4×10^3 $cm^3 \cdot mol^{-1} \cdot s^{-1}$ at 1073 K) (Cohen and Westberg, 1991), we presume that N does not contribute significantly to H_2S conversion. The N atom radicals predominantly recombine to N_2 because rate constant of R7 is about 8×10^6 higher than that of R6. In addition, no byproducts of ammonia were detected during our analysis, which confirms that the only significant products of H_2S conversion in N_2 are H_2 and S.

For H_2S-Ar-N_2 mixtures, the interaction of $Ar(^3P_2)$ with N_2 and the interaction of Ar with the excited states of N_2 can enhance H_2S decomposition. As confirmed with H_2S-Ar and H_2S-N_2 mixtures, $Ar(^3P_2)$ and $N_2(A)$ appear to be directly involved in H_2S dissociation through reactions R2 and R5, respectively. $Ar(^3P_2)$ can collide with N_2 to generate the excited state, $N_2(C)$ (Velazco et al., 1978).

$$Ar(^3P_2) + N_2 \rightarrow Ar + N_2(C) \qquad k = 2.17 \times 10^{13}\ cm^3.mol^{-1}.s^{-1} \qquad (R10)$$

$N_2(C)$ is transformed to $N_2(B)$ either through radiative emission or through collision-induced radiation.

$$N_2(C) \rightarrow N_2(B) + h\nu \qquad k = 2.73 \times 10^7\ s^{-1} \qquad (R11)$$

$$N_2(C) + Ar \rightarrow N_2(B) + h\nu \qquad k = 8.19 \times 10^{11}\ cm^3.mol^{-1}.s^{-1} \qquad (R12)$$

Any of the three reactions shown below, can lead to formation of $N_2(A)$ from $N_2(B)$. $N_2(A)$ can then directly dissociate H_2S through R5.

$$N_2(B) + N_2 \rightarrow N_2(A) + N_2 \qquad k = 1.81 \times 10^{13}\ cm^3.mol^{-1}.s^{-1} \qquad (R13)$$

$$N_2(B) + Ar \rightarrow N_2(A) + Ar \qquad k = 9.63 \times 10^{11}\ cm^3.mol^{-1}.s^{-1} \qquad (R14)$$

$$N_2(B) \rightarrow N_2(A) + h\nu \qquad k = 2.00 \times 10^5\ s^{-1} \qquad (R15)$$

Thus, in H_2S-Ar-N_2 mixtures, in addition to $N_2(A)$ formation by electron collision with N_2 (R5) as in the H_2S-N_2 mixtures, there is a parallel route (R10-R15) to form $N_2(A)$. $N_2(A)$ and $Ar(^3P_2)$ are responsible for H_2S dissociation through reactions R2 and R9. This increase in $N_2(A)$ production is the probable reason for the increase in H_2S conversion in H_2S-Ar-N_2 mixtures compared to that in H_2S-Ar or H_2S-N_2 mixtures.

3.6. Sulfur formation

Sulfur is a product of direct decomposition of H_2S. Initially, atomic sulfur is formed in high temperature areas of the discharge and then it dimerizes, forms clusters, and condenses in the low temperature zone on the discharge periphery (Fridman and Kennedy, 2004a). S and S_2 have been reported in gas discharges (Elbanowski, 1969; Meyer, 1976). Formation of sulfur clusters (S_4, S_6 and S_8) have also been reported during the microwave decomposition of H_2S (Fridman and Kennedy, 2004a). However, in the equilibrium vapor, below 400 K (close to our reactor temperature), S_8 accounts for over 90 mol% of the vapor, while S_6 and S_7 make up the rest (Meyer, 1976). The sulfur formed in the vapor phase in our reactor condenses as a grayish (sometimes grayish-yellow) deposit. All sulfur allotropes with ring structures are yellow, while the sulfur chains are dark colored (Meyer, 1976). An X-ray diffraction study of the deposit shows the presence of orthorhombic-α sulfur, indicating that the sulfur formed in our reactor is a mixture of orthorhombic-α and other allotropes.

4. Conclusions

A novel reactor design, wire-in-tube configuration with view-ports, allowed visual observation of the corona all along the length of the reactor. The H_2S conversion

and energy efficiency of H_2S decomposition in the pulsed corona discharge reactor varied greatly at a constant power. Low charge voltage, high pulse frequency, and low pulse forming capacitance operation produce the highest energy efficiency for H_2S conversion at constant power. Low charge voltage and high pulse frequency operation apparently does not produce inefficient secondary streamers, compared to high charge voltage and low pulse frequency conditions. Low pulse forming capacitance operation is closer to the optimum energy transfer condition, which allows better transfer of energy to the reactor and improves H_2S conversion and energy efficiency. The trend of increasing energy efficiency as the capacitance ratio approaches the optimum energy transfer ratio confirms these are the optimum energy transfer conditions for a high pressure, high concentration, and high flow rate system. Dilution of H_2S-Ar feed mixtures with N_2, increases the plasma volume within the reactor and may increase production of $N_2(A)$ species, which along with $Ar(^3P_2)$ appear responsible for H_2S dissociation. The lowest energy consumption for H_2S decomposition in a plasma reactor at non-vacuum pressures was obtained in an equimolar mixture of Ar and N_2 at the lowest value of pulse forming capacitance. H_2S decomposition in an equimolar mixture of Ar and N_2, combined with improved reactor geometry to optimize pulse forming capacitance for maximum energy transfer, should increase energy efficiency further.

Acknowledgements

This work was supported by the Department of Energy (DE-FC26-03NT41963), the Idaho National Laboratory Directed Research and Development (Battelle 47698), the

University of Wyoming Research Office, and the University of Wyoming School of Energy Resources. The authors gratefully acknowledge experimental assistance provided by Mr. R. Borgialli.

Figure Captions

Figure 1. Experimental setup

Figure 2. Reactor electrical circuit diagram

Figure 3. Corona discharge as seen through a viewport

Figure 4. Conversion of H_2S as a function of charge voltage and capacitance. (a) 8% H_2S – 92% Ar (b) 12% H_2S – 88% Ar
Data: 720 pF (■), 1440 pF(▲), 2160 pF (×), 2880 pF (♦)

Figure 5. Energy consumption per H_2S molecule converted as a function of charge voltage and capacitance. (a) 8% H_2S – 92% Ar (b) 12% H_2S – 88% Ar
Data: 720 pF (■), 1440 pF(▲), 2160 pF (×), 2880 pF (♦)

Figure 6. Energy consumption per H_2S molecule converted as a function of capacitance ratio at a charge voltage of 17 kV.
Data: 8% H_2S – 92% Ar (■),12% H_2S – 88% Ar (▲)

Figure 7. H_2S conversion in Ar-N_2 mixture as balance gas
Data: 100 W (♦), 80 W (■), 60 W(▲)

Figure 8. Energy consumption for H_2S decomposition in Ar-N_2 mixture as balance gas
Data: 100 W (♦), 80 W (■), 60 W(▲)

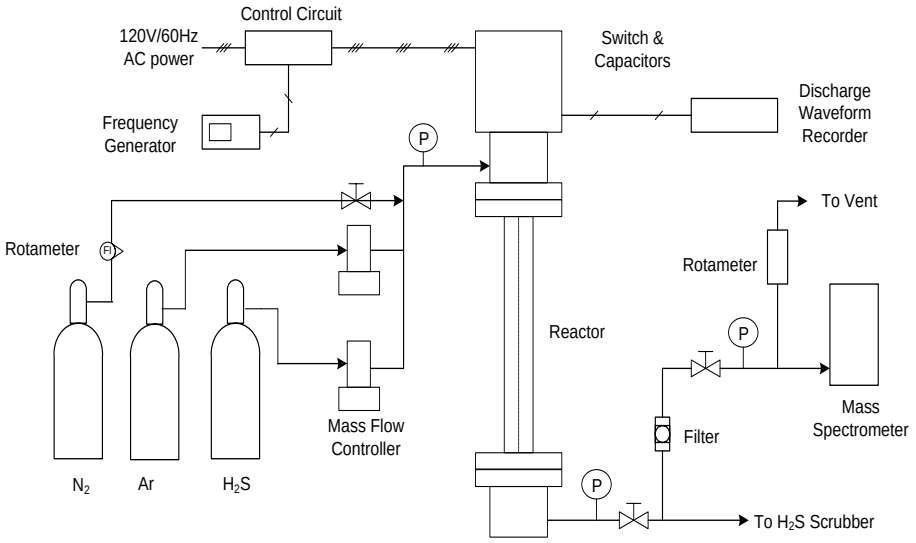

Figure 1. Experimental setup

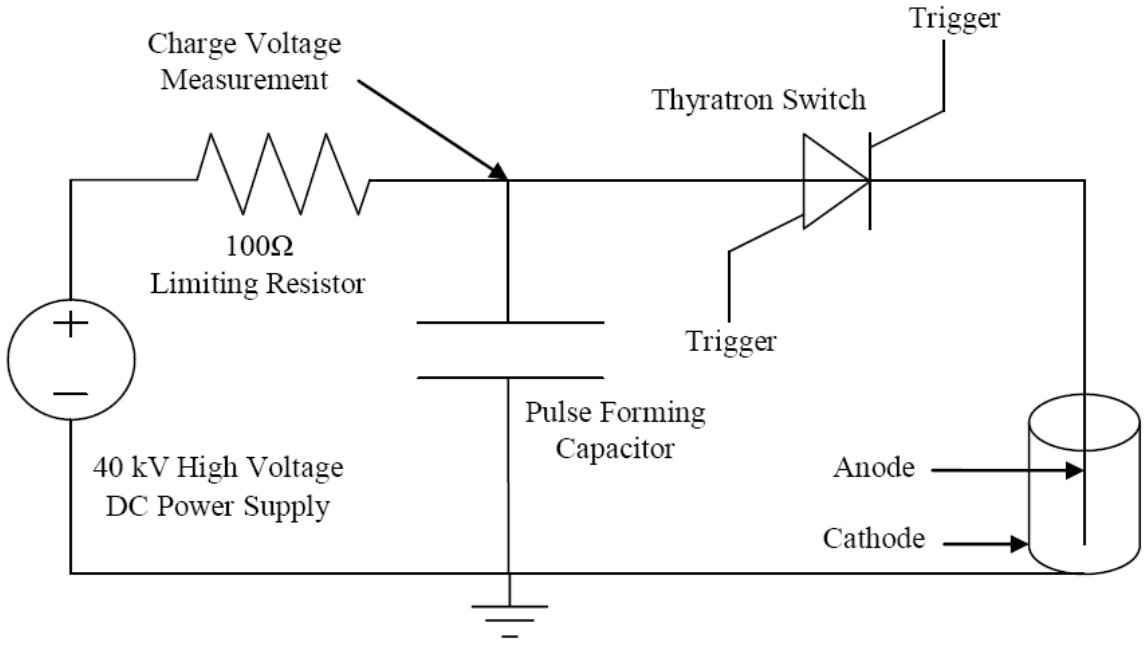

Figure 2. Reactor electrical circuit diagram

Figure 3. Corona discharge as seen through a viewport

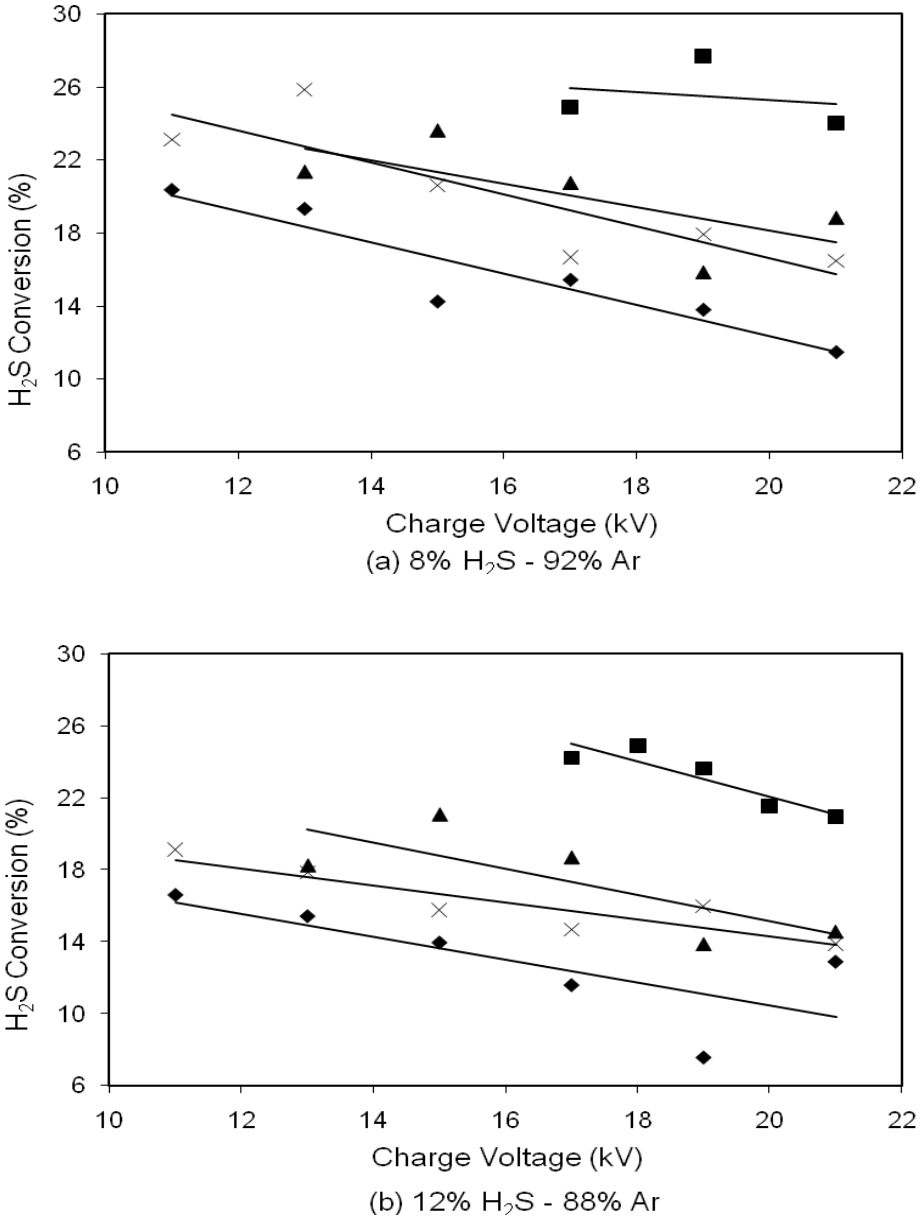

Figure 4. Conversion of H_2S as a function of charge voltage and capacitance. (a) 8% H_2S – 92% Ar (b) 12% H_2S – 88% Ar
Data: 720 pF (■), 1440 pF(▲), 2160 pF (×), 2880 pF (♦)

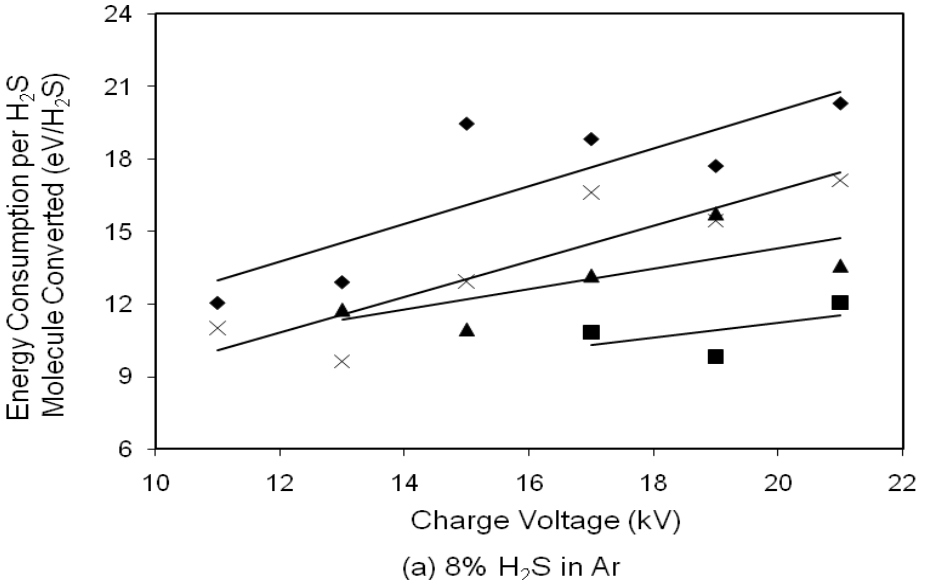

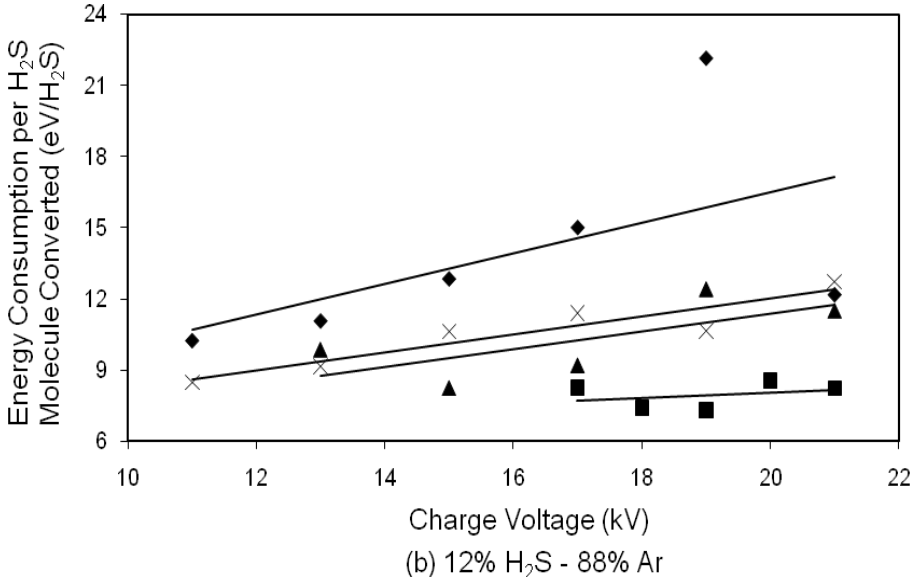

Figure 5. Energy consumption per H_2S molecule converted as a function of charge voltage and capacitance. (a) 8% H_2S – 92% Ar (b) 12% H_2S – 88% Ar
Data: 720 pF (■), 1440 pF(▲), 2160 pF (×), 2880 pF (♦)

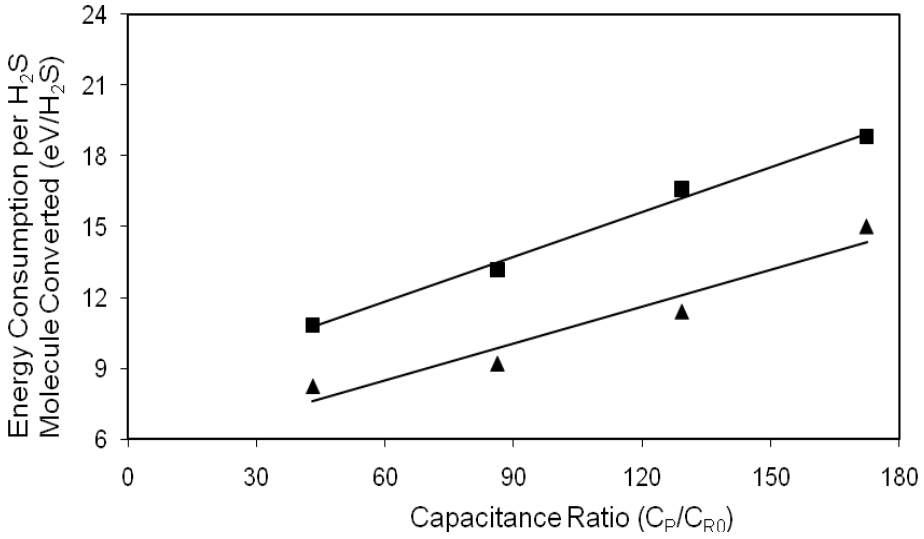

Figure 6. Energy consumption per H_2S molecule converted as a function of capacitance ratio at a charge voltage of 17 kV.
Data: 8% H_2S – 92% Ar (■),12% H_2S – 88% Ar (▲)

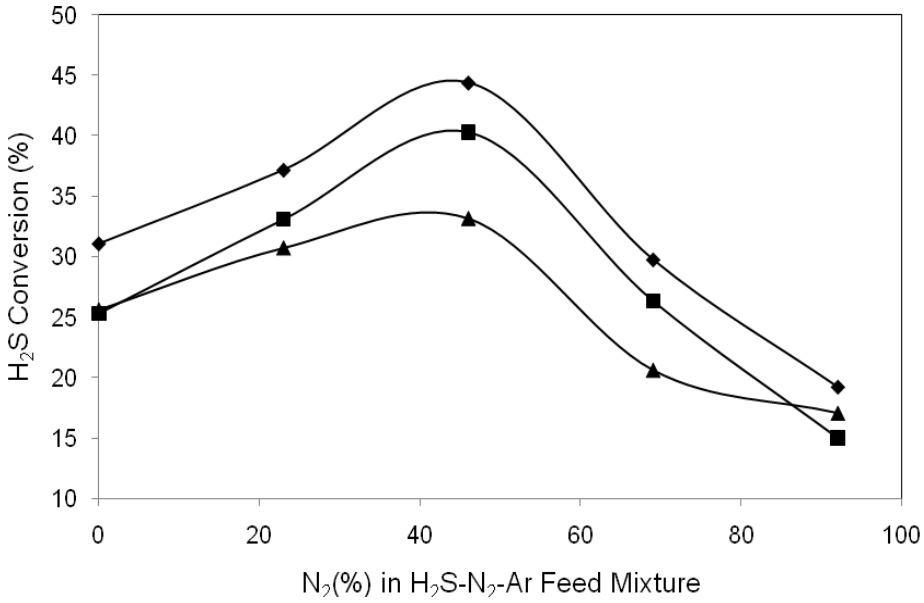

Figure 7. H_2S conversion in Ar-N_2 mixture as balance gas
Data: 100 W (♦), 80 W (■), 60 W(▲)

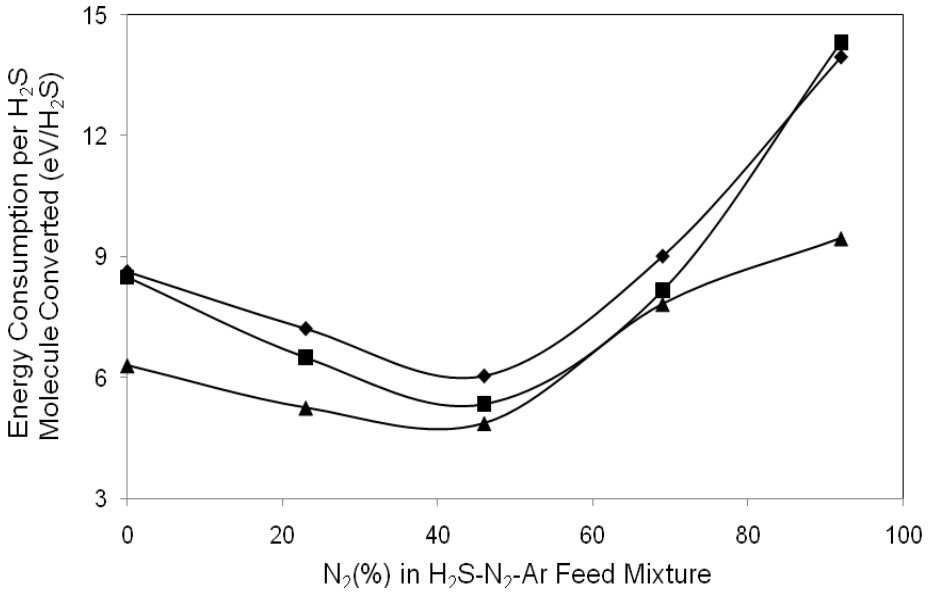

Figure 8. Energy consumption for H_2S decomposition in Ar-N_2 mixture as balance gas Data: 100 W (♦), 80 W (■), 60 W(▲)

Table Captions

Table 1. Molar composition of feed gas mixtures for experiments involving nitrogen

Table 2. Electrical parameters for constant power experiments at 100 W

Table 3. Electrical parameters for experiments involving nitrogen

Table 4. Electron collision with H_2S in primary and secondary streamers
(* denotes an excited state as proposed by (Rao and Srivastava, 1993))

Table 5. Decrease in energy consumption with decrease in capacitance ratio
(Representative data, at 17 kV)

Gas Mixture #	H_2S (%)	Ar (%)	N_2 (%)
1	8	92	0
2	8	69	23
3	8	46	46
4	8	23	69
5	8	0	92

Table 1. Molar composition of feed gas mixtures for experiments involving nitrogen

Pulse forming capacitance (C_P, pF)	Charge voltage (V, kV)					
	Pulse frequency (f, Hz)					
720	11	13	15	17	19	21
	-	-	-	961	769	630
1440	11	13	15	17	19	21
	-	822	618	481	385	315
2160	11	13	15	17	19	21
	765	548	412	320	256	210
2880	11	13	15	17	19	21
	574	411	309	240	192	157

Table 2. Electrical parameters for constant power experiments at 100 W

Power (P,W)	60	80	100
Pulse forming capacitance (C_P, pF)	720	720	720
Charge voltage (V, kV)	13	15	17
Pulse frequency (f, Hz)	986	988	961

Table 3. Electrical parameters for experiments involving nitrogen

Primary streamer processes	Approximate cross section (10^{-23} m^2)
$H_2S + e(\sim 10\ eV) \rightarrow H^* + HS^-$	0.15
$H_2S + e(\sim 10\ eV) \rightarrow 2H^*$ (or H_2^*) $+ S^-$	3.8
$H_2S + e(\sim 10\ eV) \rightarrow H_2S^+ + 2e$	100
$H_2S + e(\sim 10.45\ eV) \rightarrow H_2S^+ + 2e$	758
Secondary streamer processes	Approximate cross section (10^{-23} m^2)
$H_2S + e(2.28\ eV) \rightarrow H + HS^-$	18
$H_2S + e(2.5\ eV) \rightarrow H_2 + S^-$	3.3

Table 4. Electron collision with H_2S in primary and secondary streamers
(* denotes an excited state as proposed by (Rao and Srivastava, 1993))

Pulse forming capacitance (C_P, pF)	720	1440	2160	2880
Capacitance ratio (C_P/C_{R0})	45	90	135	180
Energy consumption in 8% H_2S-92% Ar mixture (E, eV/H_2S molecule converted)	10.8	13.2	16.6	18.8
Energy consumption in 12% H_2S-88% Ar mixture (E, eV/H_2S molecule converted)	8.2	9.2	11.4	15.0

Table 5. Decrease in energy consumption with decrease in capacitance ratio
(Representative data, at 17 kV)

References

2002, Hydrogen Thyratrons Preamble, A1A-Hydrogen Thyratrons Preamble, E2V Technologies Limited, p. 1-21.

2004, Basic Research Needs for the Hydrogen Economy, The “Basic Research Needs” Workshop Series, Argonne National Laboratory.

2005, Today's Hydrogen Production Technology, Hydrogen & Clean Fuels Research, Washington, D.C., Fossil Energy Office of Communications. http://www.fossil.energy.gov/programs/fuels/hydrogen/currenttechnology.html

2008, Chemical Profiles, The Innovation Group. http://www.the-innovation-group.com/ChemProfiles/Hydrogen.htm

Abolentsev, V. A., S. V. Korobtsev, D. D. Medvedev, B. V. Potapkin, V. D. Rusanov, A. A. Fridman, and V. L. Shiryaevskii, 1995, Pulsed wet discharge as an effective means of gas purification from H2S and organosulfur impurities: High Energy Chemistry, v. 29, p. 353-357.

Aleksandrov, E. N., V. Y. Basevich, and V. I. Vedeneev, 1994, Initial act of nitrogen atom interaction with H2 in gas-phase: Khimicheskaya Fizika, v. 13, p. 90-93.

Asisov, R. I., A. K. Vakar, A. F. Gutsol, V. K. Givotov, E. G. Krasheninnikov, M. F. Krotov, V. D. Rusanov, A. A. Fridman, and G. V. Sholin, 1985, Plasmachemical methods of energy carrier production: International Journal of Hydrogen Energy, v. 10, p. 475-477.

Averin, V. G., V. B. Potapkin, V. D. Rusanov, A. A. Fridman, and V. L. Shiryaevskii, 1996, Dissociation of hydrogen sulfide molecules in a pulsed electric discharge: High Energy Chemistry, v. 30, p. 125-127.

Bagautdinov, A. Z., V. K. Jivotov, J. I. Eremenko, I. A. Kalachev, A. I. Kozbagarov, E. I. Konstantinov, S. A. Musinov, K. I. Overchuk, V. D. Rusanon, and V. A. Zoller, 1998, Plasmachemical hydrogen production from natural gases containing hydrogen sulfide.: World Hydrogen Energy Conference, p. 683-689.

Bagautdinov, A. Z., V. K. Jivotov, J. I. Eremenko, I. A. Kalachev, S. A. Musinov, A. M. Pampushka, V. D. Rusanon, and V. A. Zoller, 1993a, Natural hydrogen sulfide (H2S)— source of hydrogen (plasma chemical dissociation): Frontier Science Series, v. 7, p. 123-125.

Bagautdinov, A. Z., V. K. Jivotov, J. I. Eremenko, I. A. Kalachev, S. A. Musinov, B. V. Potapkin, A. M. Pampushka, V. D. Rusanov, M. I. Strelkova, A. A. Fridman, and V. A. Zoller, 1995, Plasma chemical production of hydrogen from H2S-containing gases in MCW discharge: International Journal of Hydrogen Energy, v. 20, p. 193-195.

Bagautdinov, A. Z., V. K. Zhivotov, I. A. Kalachev, S. A. Musinov, A. M. Pampushka, V. D. Rusanov, and V. A. Tsoller, 1993b, Investigations of the radial distributions of gas-flows in a high-power microwave-discharge: High Energy Chemistry, v. 27, p. 305-310.

Bagautdinov, A. Z., V. K. Zhivotov, S. V. Musinov, A. M. Pampushka, V. D. Rusanov, V. A. Tsoller, and P. Y. Epp, 1992, Physical and chemical processes during the dissociation of H2S-CO2 mixtures in microwave discharges: High Energy Chemistry, v. 26, p. 55-61.

Bingyan, D., L. Jie, W. Yan, and L. Guofeng, 2005, Experimental study of streamer energy in pulsed corona discharge (Brief communication): Japanese Journal of Applied Physics, v. 44, p. 1959-1960.
Christophorou, L. G., H. Rodrigo, E. Marode, and F. Bastien, 1987, Isotopic dependencies of the dielectric strength of gases - new observations, classification, and possible origins: Journal of Physics D-Applied Physics, v. 20, p. 1031-1038.
Cohen, N., and K. R. Westberg, 1991, Chemical kinetic data sheets for high-temperature reactions. Part II: Journal of Physical and Chemical Reference Data, v. 20, p. 1211-1311.
Cox, B. G., P. F. Clarke, and B. B. Pruden, 1998, Economics of thermal dissociation of H2S to produce hydrogen: International Journal of Hydrogen Energy, v. 23, p. 531-544.
Dalaine, V., J. M. Cormier, and P. Lefaucheux, 1998a, A gliding discharge applied to H2S destruction: Journal of Applied Physics, v. 83, p. 2435-2441.
Dalaine, V., J. M. Cormier, S. Pellerin, and P. Lefaucheux, 1998b, H2S destruction in 50 Hz and 25 kHz gliding arc reactors: Journal of Applied Physics, v. 84, p. 1215-1221.
Elbanowski, M., 1969, Flash photolysis of sulfur vapor: Roczniki Chemii, v. 43, p. 1883-1890.
Fridman, A., and L. A. Kennedy, 2004a, Plasma Physics and Engineering: New York, Taylor & Francis, 771 p.
Fridman, A., and L. A. Kennedy, 2004b, Plasma Physics and Engineering: New York, Taylor & Francis, 42 p.
Fridman, A., and L. A. Kennedy, 2004c, Plasma Physics and Engineering: New York, Taylor & Francis, 99 p.
Fridman, A., and L. A. Kennedy, 2004d, Plasma Physics and Engineering: New York, Taylor & Francis, 75 p.
Gundel, L. A., D. W. Setser, M. A. A. Clyne, J. A. Coxon, and W. Nip, 1976, Rate constants for specific product channels from metastable Ar(P-3(2,0) reactions and spectrometer calibration in vacuum ultraviolet: Journal of Chemical Physics, v. 64, p. 4390-4410.
Haas, L. A., and S. E. Khalafalla, 1973, Decomposition of hydrogen sulfide in an electrical discharge, Report of Investigations, Washington, D.C., Twin Cities Metallurgy Research Center, p. 1-21.
Helfritch, D. J., 1993, Pulsed corona discharge for hydrogen-sulfide decomposition: Ieee Transactions on Industry Applications, v. 29, p. 882-886.
Herron, J. T., 1999, Evaluated chemical kinetics data for reactions of N(D-2), N(P-2), and N2(A(3)Sigma(+)(u)) in the gas phase: Journal of Physical and Chemical Reference Data, v. 28, p. 1453-1483.
Huang, C. P., and A. T-Raissi, 2008, Liquid hydrogen production via hydrogen sulfide methane reformation: Journal of Power Sources, v. 175, p. 464-472.
Kossyi, I. A., A. Y. Kostinsky, A. A. Matveyev, and V. P. Silakov, 1992, Kinetic scheme of the non-equilibrium discharge in nitrogen-oxygen mixtures: Plasma Sources Science and Technology, v. 1, p. 207-220.
Lide, D. R., Ed., 2003, CRC Handbook of Chemistry and Physics: CRC Handbook of Chemistry & Physics: Boca Raton, CRC Press LLC, 9-66 p.

Ma, H., P. L. Chen, and R. Ruan, 2001, H2S and NH3 removal by silent discharge plasma and ozone combo system: Plasma Chemistry and Plasma Processing, v. 21, p. 611-624.
Meyer, B., 1976, Elemental sulfur: Chemical Reviews, v. 76, p. 367-388.
Mok, Y. S., 2000, Efficient energy delivery condition from pulse generation circuit to corona discharge reactor: Plasma Chemistry and Plasma Processing, v. 20, p. 353-364.
Rao, M. V. V. S., and S. K. Srivastava, 1993, Electron impact ionization and attachment cross sections for H2S: Journal of Geophysical Research, v. 98, p. 13137-13145.
Ruan, R. R., W. Han, A. Ning, P. L. Chen, P. R. Goodrich, and R. Zhang, 1999, Treatment of odorous and hazardous gases using non-thermal plasma: Journal of Advanced Oxidation Technologies, v. 4, p. 328-332.
Shin, D. N., C. W. Park, and J. W. Hahn, 2000, Detection of OH(A(2)Sigma(+)) and O(D-1) emission spectrum generated in a pulsed corona plasma: Bulletin of the Korean Chemical Society, v. 21, p. 228-232.
Smith, J. M., and H. C. Van Ness, 1987, Introduction to Chemical Engineering Thermodynamics: McGraw-Hill Chemical Engineering Series: Singapore, McGraw-Hill Book Company, 121 p.
Szmytkowski, C., P. Mozejko, and A. Krzysztofowicz, 2003, Measurements of absolute total cross sections for electron scattering from triatomic polar molecules: SO2 and H2S: Radiation Physics and Chemistry, v. 68, p. 307-311.
Traus, I., and H. Suhr, 1992, Hydrogen-sulfide dissociation in ozonizer discharges and operation of ozonizers at elevated-temperatures: Plasma Chemistry and Plasma Processing, v. 12, p. 275-285.
Traus, I., H. Suhr, J. E. Harry, and D. R. Evans, 1993, Application of a rotating high-pressure glow-discharge for the dissociation of hydrogen-sulfide: Plasma Chemistry and Plasma Processing, v. 13, p. 77-91.
Uhm, H. S., and W. M. Lee, 1997, An analytical theory of corona discharge plasmas: Physics of Plasmas, v. 4, p. 3117-3128.
Velazco, J. E., J. H. Kolts, and D. W. Setser, 1978, Rate constants and quenching mechanisms for metastable states of argon, krypton, and xenon: Journal of Chemical Physics, v. 69, p. 4357-4373.
Watson, J. T., 1997, Introduction to Mass Spectrometry: Philadelphia, Lippincott-Raven.
Winands, G. J. J., Z. Liu, A. J. M. Pemen, E. J. M. van Heesch, K. Yan, and E. M. van Veldhuizen, 2006, Temporal development and chemical efficiency of positive streamers in a large scale wire-plate reactor as a function of voltage waveform parameters: Journal of Physics D-Applied Physics, v. 39, p. 3010-3017.
Wiseman, N., and W. J. M. Douglas, 1972, Oxidation of hydrogen sulfide in a corona discharge: A. I. Ch. E. Symposium Series, v. 68, p. 297-301.
Yan, K. P., H. X. Hui, M. Cui, J. S. Miao, X. L. Wu, C. G. Bao, and R. N. Li, 1998, Corona induced non-thermal plasmas: Fundamental study and industrial applications: Journal of Electrostatics, v. 44, p. 17-39.
Yao, S. L., A. Nakayama, and E. Suzuki, 2001, Methane conversion using a high-frequency pulsed plasma: Discharge features: A.I.Ch.E. Journal, v. 47, p. 419-426.

Zhao, G. B., M. D. Argyle, and M. Rodosz, 2006a, Effect of CO on NO and N2O conversions in nonthermal argon plasma: Journal of Applied Physics, v. 99.
Zhao, G. B., S. B. J. Garikipati, X. D. Hu, M. D. Argyle, and M. Radosz, 2005a, The effect of gas pressure on NO conversion energy efficiency in nonthermal nitrogen plasma: Chemical Engineering Science, v. 60, p. 1927-1937.
Zhao, G. B., S. V. B. Garikipati, X. D. Hu, M. D. Argyle, and M. Radosz, 2005b, Effect of oxygen on nonthermal plasma reactions of nitrogen oxides in nitrogen: A.I.Ch.E. Journal, v. 51, p. 1800-1812.
Zhao, G. B., X. D. Hu, M. D. Argyle, and M. Radosz, 2004, N atom radicals and N-2(A(3)Sigma(+)(u)) found to be responsible for nitrogen oxides conversion in nonthermal nitrogen plasma: Industrial & Engineering Chemistry Research, v. 43, p. 5077-5088.
Zhao, G. B., X. D. Hu, M. D. Argyle, and M. Radosz, 2005c, Effect of CO2 on nonthermal-plasma reactions of nitrogen oxides in N-2. Part II: Percent-level concentrations: Industrial & Engineering Chemistry Research, v. 44, p. 3935-3946.
Zhao, G. B., S. John, J. J. Zhang, J. C. Hamann, S. S. Muknahallipatna, S. Legowski, J. F. Ackerman, and M. D. Argyle, 2007, Production of hydrogen and sulfur from hydrogen sulfide in a nonthermal-plasma pulsed corona discharge reactor: Chemical Engineering Science, v. 62, p. 2216-2227.
Zhao, G. B., S. John, J. J. Zhang, L. N. Wang, S. Muknahallipatna, J. C. Hamann, J. F. Ackerman, M. D. Argyle, and O. A. Plumb, 2006b, Methane conversion in pulsed corona discharge reactors: Chemical Engineering Journal, v. 125, p. 67-79.